HHS Public Access

Author manuscript

J Allergy Clin Immunol. Author manuscript; available in PMC 2017 September 01.

Published in final edited form as:

J Allergy Clin Immunol. 2016 September ; 138(3): 825–838. doi:10.1016/j.jaci.2015.12.1330.

Clonal expansion of CD4+ Cytotoxic T Lymphocytes in IgG4-related disease

Hamid Mattoo, PhD[1,†], **Vinay S. Mahajan, MBBS, PhD**[1,†], **Takashi Maehara, DDS, PhD**[1,2], **Vikram Deshpande, MD**[1], **Emanuel Della-Torre, MD**[1], **Zachary S. Wallace, MD**[1], **Maria Kulikova, BS**[1], **Jefte M. Drijvers, MD**[1], **Joe Daccache, BS**[1], **Mollie N. Carruthers, MD**[1], **Flavia Castellino, MD**[1], **James R. Stone, MD, PhD**[1], **John H. Stone, MD, MPH**[1], and **Shiv Pillai, MBBS, PhD**[1,*]

[1]Massachusetts General Hospital, Harvard Medical School, Boston MA

[2]Section of Oral and Maxillofacial Oncology, Division of Maxillofacial Diagnostic and Surgical Sciences, Fukuoka, Japan

Abstract

Background—IgG4-related disease (IgG4-RD) is a systemic condition of unknown etiology, characterized by highly fibrotic lesions with dense lymphoplasmacytic infiltrates. $CD4^+$ T cells constitute the major inflammatory cell population in IgG4-RD lesions.

Objective—We used an unbiased approach to characterize $CD4^+$ T cell subsets in IgG4-RD subjects based on their clonal expansion and their ability to infiltrate affected tissue sites.

Methods—We used flow cytometry to identify $CD4^+$ effector/memory T cells (T_{EM}) in a cohort of 101 IgG4-related disease (IgG4-RD) patients. These expanded cells were characterized by gene expression analysis and flow cytometry. Next-generation sequencing of the T cell receptor β chain gene was performed on $CD4^+SLAMF7^+$ CTLs and $CD4^+GATA3^+$ T_H2 cells in a subset of patients to identify their clonality. Tissue infiltration by specific T cells was examined using quantitative multi-color imaging.

Results—$CD4^+$ effector/memory T cells with a cytolytic phenotype were expanded in IgG4-RD patients. Next-generation sequencing revealed prominent clonal expansions of these $CD4^+$CTLs but not $CD4^+GATA3^+$ memory T_H2 cells in subjects with IgG4-RD. The dominant T cells infiltrating a range of inflamed IgG4-RD tissue sites were clonally-expanded $CD4^+$CTLs that expressed SLAMF7, granzyme A, IL-1β, and TGF-β1. Clinical remission induced by rituximab-mediated B cell depletion was associated with a reduction in disease-associated $CD4^+$ CTLs

*To whom correspondence should be addressed: Shiv Pillai, pillai@helix.mgh.harvard.edu, Ragon Institute of MGH, MIT and Harvard, 400 Tech Square, Cambridge, MA 02139 or John H. Stone, jhstone@partners.org, Rheumatology Unit, Yawkey 2, Massachusetts General Hospital, 55 Fruit Street, Boston, MA 02114.

†These authors contributed equally

Conflict of Interest

The authors declare that they have no relevant conflict of interest.

Conclusions—IgG4-RD is prominently linked to clonally-expanded, IL-1β, and TGF- β1 secreting, $CD4^+$ CTLs in peripheral blood as well as in inflammatory tissue lesions. These active, terminally-differentiated, cytokine-secreting effector $CD4^+$ T cells are now linked to a human disease characterized by chronic inflammation and fibrosis.

Keywords

Fibrosis; IgG4-related disease; IgG4; CD4+ cytotoxic T cells; T_H2 cells; rituximab; IL-1β

Introduction

IgG4-related disease (IgG4-RD) is a chronic inflammatory syndrome whose pathogenesis is poorly understood. This disease can affect virtually every organ system of the body and is characterized by tumefactive lesions, storiform fibrosis, obliterative phlebitis and the presence of IgG4 secreting plasma cells in affected tissues [1–3]. IgG4 itself is generally considered to be a non-inflammatory immunoglobulin due to its limited ability to fix complement and bind activating Fc receptors [4, 5]. There is very limited evidence that the autoantibodies described so far are of the IgG4 subclass and it is unclear whether they are involved in disease pathogenesis [6]. On the other hand, T cells are the most abundant cells in the lymphoplasmacytic infiltrate in IgG4-RD lesions and are thought to be the drivers of IgG4-RD pathogenesis[2, 3]. The analysis of circulating T_H1 and T_H2 cells has led to conflicting results in IgG4-RD subjects. One study reported a T_H1 skew in peripheral blood T cells in autoimmune pancreatitis while other studies on IgG4-related sialoadenitis showed an increase in cells expressing Th2 cytokines in peripheral blood [7–10]. Some T_H2 type cytokines as well as M2 macrophages have been found in IgG4-RD lesions suggesting that this disease may be caused by T_H2 cells [11]. We have recently reported that atopic manifestations are seen in about 40% of IgG4-RD subjects, a proportion that is within the range seen in the population at large [12]. We also performed studies on GATA-3 expressing circulating T_H2 cells in IgG4-RD subjects. Circulating GATA-3^+ IL-4, IL-5 and IL-13 secreting T_H2 cells were only found in IgG4-RD subjects with a history of atopy [13].

Fibrosis is a prominent feature of many chronic inflammatory disorders, including rheumatoid arthritis, systemic sclerosis, systemic lupus erythematosus and IgG4-related disease among others. Many distinct triggers are known to contribute to fibrosis, but a detailed understanding of this pathological process has proved elusive [14]. Both innate and adaptive immune mechanisms may drive fibrotic responses [15] but it is unclear what constitutes the tipping point between physiological wound healing and pathological fibrosis. Activated macrophages secrete cytokines such as tumor necrosis factor alpha (TNF-α) and interleukin-1β (IL-1β) that activate fibroblasts and induce the overproduction of extracellular matrix (ECM) proteins [15]. In the murine model of bleomycin-induced pulmonary fibrosis, inflammasome activation and IL-1R/MyD88 signaling are critical aspects of the profibrotic activity of IL-1β [16]. Transient expression of IL-1β alone in the rat lung has been shown to result in tissue damage and progressive fibrosis [17]. Transgenic overexpression of IL-1β in the murine pancreas also results in a fibrotic pancreatitis [18].

Numerous studies have implicated the type 2 cytokines, IL-4, IL-5 and IL-13, in driving progressive fibrosis [19]. IL-4 can directly induce mouse and human fibroblasts to synthesize ECM proteins [19–21]. IL-13, secreted by T_H2 cells, mediates fibrotic remodeling in a TGF-β1 dependent or independent manner in experimental lung fibrosis, and may contribute to the pathogenesis of idiopathic pulmonary fibrosis, systemic sclerosis, dermatitis induced skin fibrosis and liver fibrosis associated with persistent infections [22–27]. M2 macrophages that have been triggered by IL-4 and IL-13 can induce other cells to produce IL-4, IL-10, IL-13 and TGF-β1 and thus contribute to fibrosis. M2 macrophages involved in wound healing also secrete large amounts of TGF-β1 [28], a cytokine that has also been linked to the genesis of fibrosis. Although fibrosis is generally linked to what is presumably the uncontrolled activity of T_H2 cells, M2 macrophages and fibroblasts, the prominent role in fibrosis of IL-1β, a cytokine typically made by M1 macrophages, suggests that such T_H2 biased models may be applicable to a subset of fibrotic diseases. The presumption that a number of fibrotic diseases have an underlying T_H2 origin may be an oversimplification of an otherwise complex and poorly understood pathogenic processes.

Because expansions of circulating T_H2 cells were not observed in IgG4-RD subjects without atopy, we undertook an unbiased approach using next-generation sequencing to study the clonality of effector $CD4^+$ T cells in patients with active untreated IgG4-RD. Our goal was to identify any specific $CD4^+$ effector sub-population that is clonally expanded in subjects with this disease. We report here that $CD4^+$ T cells with a cytotoxic T lymphoid phenotype are clonally expanded in IgG4-RD subjects. Further these unusual $CD4^+$ T cells can synthesize and secrete IFN-γ, IL-1β and TGF- β1 following TCR or TLR triggering. In addition to these cells being expanded in the blood, they are also found as the dominant $CD4^+$ T cell population within diseased tissue sites where they also synthesize cytokines. Their numbers decline concomitant with a clinical response to rituximab therapy, suggesting a contributory role for these $CD4^+SLAMF7^+$ cytotoxic T cells in the pathogenesis of this systemic fibrotic disease. We have also observed $CD4^+$ CTL expansions in a smaller cohort with systemic sclerosis. Our data therefore suggest that IFN-γ, IL-1β and TGF-β1 secreting $CD4^+$ CTLs contribute to the pathogenesis of IgG4-RD and are likely to be of broader relevance in other inflammatory fibrotic disorders.

Materials and Methods

Patients

We evaluated the peripheral blood from 101 IgG4-RD patients and selected tissue samples from a subset of those followed at the Massachusetts General Hospital (MGH). This study was approved by the Partners Institutional Review Board. All subjects provided written informed consent. Data pertaining to demographics, prior treatment, and laboratory findings at baseline evaluations were derived from MGH Autoimmune Disease Center of Excellence for IgG4-RD and the medical record. All patients had biopsies from at least one organ that were reviewed and confirmed at our center. For certain analyses, only patients with active, untreated disease at sampling were included. Confirmation of the IgG4-RD diagnosis was predicated upon both specific histopathologic features and an increased number of $IgG4^+$

plasma cells (or increased $IgG4^+/IgG^+$ ratio) in affected tissues [29]. Data from IgG4-RD patients were compared with 35 healthy controls (age 32–70 years).

Tissue sections from 5 IgG4-related dacryoadenitis and sialadenitis (i.e., IgG4-related Mikulicz disease) subjects (mean age = 68.6 ±4.12) and 5 Sjögren's syndrome patients (mean age = 50.8 ± 9.14) obtained from Department of Oral and Maxillofacial Surgery, Kyushu University Hospital, Fukuoka, were also studied.

A subset of 74 IgG4-RD patients that met the definitions of the European Academy of Allergy and Clinical Immunology[30] were categorized based on their atopic history (Supplementary table 1). Seventeen patients with systemic sclerosis (age 24–85 yrs, median = 51 yrs; Supplementary table 2) were also chosen for this study.

Flow cytometry methods

Please see Appendix for detailed laboratory methods. Briefly, flow cytometry was performed by incubating cells in staining buffer (Biolegend) containing optimized concentrations of fluorochrome-conjugated antibodies. Surface staining was performed at 4°C for 30 minutes. For intracellular staining of transcription factors (T-bet, GATA-3, and Foxp3), cytokines (IFNγ and IL-4) as well as cytolytic molecules (granzyme B and perforin) cells were fixed and permeabilized with the Foxp3-staining kit (eBioscience) according to the manufacturer's guidelines. Cells were then stained in permeabilization buffer at 4°C for 45 minutes. Stained samples were analyzed on a BD LSR II and sorted on a BD FACSAria II (BD Biosciences).

Methods for next generation sequencing

Next-generation sequencing analysis of the TCR Vβ repertoire was undertaken using the ImmunoSeq® platform (Adaptive Biotechnologies), designed to target an output of 200,000 assembled output sequences [31, 32].

Gene expression analysis

The nCounter® human immunology panel (NanoString Technologies) was used to quantify the gene expression of effector/memory CD4+ T cells. Targets were reverse-transcribed and pre-amplified for 14 cycles using the standard multiplexed target enrichment protocol for 458 immunology-related target genes, previously validated to yield a linear response. The amplified products were hybridized in solution to color-coded nCounter probes, captured on an nCounter Cartridge for high-resolution digital scanning, and analyzed on the GEN2 Digital Analyzer. Detailed methodology is included in Supplementary Appendix 1 at www.jacionline.org

Results

Clinical data

Clinical data on the 101 patients with IgG4-RD are shown in Table 1. Of the 101 patients, 61.4% were male and 75% were of European descent. The average age of disease onset was 51.63 years (± 15.3). About 53.5% patients had elevated serum IgG4 levels at baseline. Our IgG4-RD patient cohort represented untreated patients with diverse presentation of the

disease with some patients showing a localized single organ disease (like salivary gland involvement and lung disease) while others showed a more systemic multi-organ disease (pancreas, kidney, lung, skin etc). As reported earlier, around 45% of IgG4-RD patients had a history of atopy[33] (Supplementary table 1).

Effector memory T cells with cytolytic and myeloid features are expanded in IgG4-RD

We have previously reported that Th2 cells are seen in the circulation only in a subset of IgG4-RD patients with concomitant apotic disease[13]. We corroborated these findings on atopic and non-atopic IgG4-RD subjects in this larger cohort of IgG4-RD patients (Fig E1). We sought to investigate IgG4-RD subjects with active disease in an unbiased way by looking for the presence of $CD4^+$ T-cell populations that have an effector/memory phenotype presumably resulting from persistent antigenic stimulation [34, 35]. We initially performed in-depth studies on four active, untreated IgG4-RD subjects. Although all four had biopsy-proven IgG4-RD, their clinical features differed substantially. P2 had lung and kidney involvement, P12 presented with submandibular gland disease with lymph node involvement, P19 had lesions in the pancreas and submandibular glands and also had retroperitoneal fibrosis, and P25 had widespread disease with involvement of the lacrimal glands, the parotid, sublingual and submaxillary glands, the kidney, lungs, skin and prostate. We observed a striking increase in the proportion and number of $CD4^+$ $CD27^{lo}CD62L^{lo}$ T cells in all four patients (Fig 1, A). $CD4^+$ $CD27^{lo}CD62L^{lo}$ cells are all $CD45RO^+$ (Fig E2) and represent $CD4^+$ T effector/memory (T_{EM}) cells, which presumably arise from persistent exposure to auto-antigens or environmental antigens[34, 36]. The presence of regulatory T cells in tissue lesions has been documented in subjects with IgG4-related pancreatitis, sialadenitis and cholangitis [7, 9, 36]. However, we observed only a marginal increase in circulating regulatory T cells that were identified as $CD4^+CD45RO^+CD39^+CD25^+$ $Foxp3^+$ cells in our cohort of IgG4-RD subjects; this difference was not statistically significant when compared to controls (Fig E3). Given the significant increase of $CD4^+$ T_{EM} cells in IgG4-RD patients compared to healthy controls (Fig 1, B), we decided to characterize these cells further and investigate their abundance and potential pathogenic role in IgG4-RD.

We profiled the expression of a selected panel of genes in this expanded pool of $CD4^+$ T_{EM} cells in the four patients described above. Similar gene expression profiles were seen in all 4 patients (Fig 1, C). A modified Th1 gene signature was observed, with increased expression of the transcription factor T-bet along with co-expression of genes encoding two SLAM family members, SLAMF7 and 2B4. A number of genes encoding cytolytic proteins including perforin, granzyme A, granzyme B, and granulysin were also expressed at high levels. Moreover, these T cells exhibited a distinct myeloid signature with increased expression of genes encoding CD11b, CMKLR1, IL-1β, and CCL4.

Disease-related T_{EM} cells are functional cytolytic cells

The expression of many of the differentially expressed genes in T_{EM} cells was validated at the protein level using flow cytometry and a large proportion of the expanded $CD4^+$ T_{EM} cells in PBMCs of disease subjects co-expressed SLAMF7, perforin, granzyme B and T-bet (Fig 2, A). The above markers were also found to be co-expressed in a single expanded clone identified using the corresponding TCR Vβ-specific antibody, suggesting that the

expanded clones represent a uniformly differentiated sub-population that can be tracked by the expression of SLAMF7 and T-bet (Fig 2, B). These cells appear to be phenotypically identical to previously reported $CD4^+$CTLs seen in chronic viral infections[11, 37]. These clonally expanded $CD4^+$CTLs maintained their phenotype in vitro when cultured in the presence of anti-CD3/anti-CD28 beads and recombinant human IL-2 (20 ng/mL) (Fig E4).

The $CD4^+$ CTLs seen in IgG4-RD subjects bear a striking resemblance to cytotoxic $CD4^+$ T lymphocytes reported in mice in the context of chronic antigenic stimulation [38]. The development of these cells in mice is associated with the gain of Eomes and Runx3 and the loss of ThPOK expression [38]. Like the murine $CD4^+$ CTLs, $CD4^+SLAMF7^+$ T cells from IgG4-RD patients exhibited decreased levels of ThPOK and increased expression of Runx3 when compared to $CD4^+CD45RA^+$ naïve cells and $CD4^+CD45RO^+$ memory cells from healthy controls (Fig 2, C). These cells also express surface CD8α as has been reported in mice (Fig E5) [38].

These $CD4^+$ $SLAMF7^+$ T cells cells have potent cytolytic function; upon in vitro stimulation with anti-CD3, these cells undergo degranulation as inferred from the surface expression of CD107a (Fig 2, D) and exhibit cytotoxic activity against allogeneic EBV-transformed B cell targets (Fig 2, E and Fig E6).

Circulating $CD4^+SLAMF7^+$ CTLs exhibit large clonal expansions while $CD4^+GATA3^+$ T_H2 cells in IgG4-RD subjects are clonally diverse

In order to identify potentially pathogenic subsets of $CD4^+$ T_{EM} cells that were clonally expanded in response to a potential antigen, we analyzed their TCRβ chain gene rearrangements using next-generation sequencing. We initially analyzed the TCRβ chain gene repertoire of $CD4^+$ CTLs from four untreated subjects with active, biopsy-proven IgG4-RD with distinct clinical features. We found that $CD4^+$ CTLs were oligoclonally expanded, typically with a single dominant clone representing 15% to 50% of all the in-frame V-D-J rearrangements detected (Figs 3, A and B). Several minor clones were also seen in each patient. In contrast, the repertoire of $CD4^+$ T cells from 4 healthy controls analyzed was highly diverse and no dominant clones were observed in these individuals (Fig 3, A and Fig E7, A). The Vβ-Jβ gene segment usage of the most expanded clones was not identical across IgG4-RD subjects and there were no clones with shared CDR3 sequences across individuals; disease subjects have diverse MHC class II alleles (data not shown). The TCR Vβ gene usage in a subset of expanded $CD4^+$ CTL clones as determined by next-generation sequencing was validated using TCR Vβ-specific antibodies in all 3 subjects for whom Vβ-specific antibodies could be obtained (Fig E7, B and C).

In four atopic IgG4-RD subjects (P3, P10, P39 and P54), in whom circulating $CD4^+GATA3^+$ memory Th2 cells as well as $CD4^+SLAMF7^+$ CTLs were expanded, we performed massively parallel sequencing of the T cell receptor (TCR)-Vβ chain to investigate clonal diversity of these CD4+ T cell subsets. $CD4^+SLAMF7^+$ CTLs were highly oligoclonal with one or a few expanded clones representing up to ~80% of the productive sequencing reads (Fig 3, B). In contrast, when analyzing simultaneously expanded GATA-3+ $CD4^+$ T cells, even the most expanded clones represented < 2% of the sequencing reads in all four subjects. These data strongly imply that $CD4^+SLAMF7^+$ CTLs have expanded in response

to a specific causal antigen, and may thus have a direct role in disease pathogenesis. In contrast, the repertoire of T_H2 phenotype cells may reflect the accumulated T cell memory acquired over time against a wide range of environmental allergens.

$CD4^+SLAMF7^+$ CTLs can be identified both in the circulation and in fibrotic lesions

$CD4^+SLAMF7^+$ CTLs cells were elevated in the peripheral blood of 101 IgG4-RD subjects studied compared to healthy controls ($p < 0.01$) (Fig 4, A & Fig E8). Unlike circulating GATA-3^+ T_H2 memory cells, $CD4^+$ $SLAMF7^+$ CTLs were abundant both in patients with and without atopy (Fig E9). A segment of diseased aorta obtained at autopsy from a previously described patient (P51), who succumbed to IgG4-RD showed the presence of $CD4^+SLAMF7^+$ cells in the vessel wall by flow cytometric analysis (Fig 4, B) [39]. Similarly, $CD4^+$ $SLAMF7^+$ cells were also detected in the biopsy of the involved nasal septum from a patient (P43) with IgG4-related midline destructive lesion (Fig 5, B)[40].

We quantitatively analyzed tissue sections from the affected organs of 10 IgG4-RD patients for whom well-preserved biopsies were available, for the presence of $GATA3^+$ T_H2 cells and $SLAMF7^+$ $CD4^+$ CTLs. The organs studied included submandibular glands (2 patients), lymph nodes (3 patients), and nasal palate/septum, retroperitoneal masses, kidney and lung (1 patient each). In these affected organs, infiltrating $CD4^+SLAMF7^+$ CTLs vastly outnumbered the sparse $CD4^+GATA3^+$ T_H2 T cells in all the IgG4-RD subjects studied, including both atopic and non-atopic individuals (Fig 4, C and D). These data suggest that T_H2 cells are unlikely to be the primary drivers of pathogenicity in IgG4-RD while $CD4^+$ CTLs appear, by all criteria examined, to be intimately linked to the pathogenesis of this disease. Abundance of $CD4^+SLAMF7^+$ CTLs in IgG4-RD lesions was also confirmed in the affected organs of 20 IgG4-RD subjects (Fig E10, A). In one subject with IgG4-RD (P25) the expanded $V\beta17^+$ T_{EM} cell clone that was dominant in the circulation (Fig 2, A) was also found to be abundant in an inflamed tissue site (Fig E10, B). $CD4^+SLAMF7^+$ CTLs also expressed granzyme A in IgG4-RD disease lesions (Fig E11). These data suggest that expanded $CD4^+$ CTLs are abundant in involved tissues and may be directly involved in the pathogenesis of IgG4-RD.

$CD4^+SLAMF7^+$ CTLs secrete profibrotic cytokines: IFNγ, IL-1β and TGF-β1

In order to understand the functional behavior of the disease-related $CD4^+$ CTLs, peripheral blood mononuclear cells were briefly re-stimulated with PMA and ionomycin to mimic TCR signaling, followed by intracellular staining for T-bet, IFN-γ and IL-4. Since T-bet is a lineage-determining transcription factor that is exclusively expressed in all the clonally expanded $CD4^+$ CTLs in IgG4-RD subjects (Fig 2, A and B), we identified re-stimulated $CD4^+$ CTLs among total $CD4^+$ lymphocytes using T-bet staining. We did not identify any T-bet^+ cells that lacked the expression of perforin or granzyme B, and which could therefore represent bona fide Th1 cells, in these patients (Fig 2, A and B). Re-stimulated $CD4^+$ CTLs cells from all IgG4-RD patients made large amounts of IFN-γ but no IL-4 (Fig. 5A). Clonally expanded $CD4^+$ CTLs, identified using specific TCR Vβ antibody staining, consistently expressed IFN-γ but not IL-4 upon re-stimulation (Fig E12).

IL-1β was the most prominent cytokine at the mRNA level in the expanded T_{EM} population. We also analyzed IL-1β at the protein level along with other cytokines more typically seen in effector T cells. Human $CD4^+$ T cells are known to express pro-IL-1β that gets processed and secreted as bioactive IL-1β upon LPS stimulation [41]. We sought to determine if $CD4^+SLAMF7^+$ cells release the processed form of IL-1β following stimulation. Upon in vitro re-stimulation with PMA and ionomycin, IL-1β producing cells were more abundant in flow-sorted $CD4^+CD45RO^+$ T cells from IgG4-RD subjects as detected by ELISPOT analysis compared to $CD4^+CD45RO^+$ T cells from healthy controls (Fig 5, B). Flow-sorted $CD4^+$ CTLs cells contained more IL-1β producing cells compared to naïve $CD4^+CD45RA^+$ T cells from four IgG4-RD subjects tested (Fig 5, C). These cells could be expanded in vitro and maintained in IL-2 with intermittent TCR stimulation without a loss of phenotype (Fig E4). The expanded $CD4^+$ CTLs retained their SLAMF7 expression and cytotoxic markers and were found to secrete the processed form (17 kDa) of IL-1β upon re-stimulation with either anti-CD3 or LPS as determined by Western blot analysis of culture supernatants (Fig 5, D). The amount of IL-1β secreted was comparable to the amount secreted by myeloid cells exposed to LPS.

Given the role of TGF-β1 in many fibrotic diseases, we examined the ability of $CD4^+$ CTLs to make TGF-β1 ex vivo as well as at sites of disease. Upon in vitro stimulation, flow sorted $CD4^+$ CTLs secreted large amounts of TGF-β1 compared to the naïve $CD4^+$ cells from the same patients (Fig 5, E).

Multi-color immunofluorescence staining of the affected organs of 22 IgG4-RD subjects showed high expression of IL-1β in a large proportion of $CD4^+$ $SLAMF7^+$ cells (Fig 6, A, and Fig E13). Furthermore, a large number of $CD4^+$ TGF-$\beta1^+$ T cells were detected in biopsies at the site of IgG4-RD lesions (Fig 6, B and Fig E14). These data suggest that $CD4^+$ CTLs have a pro-fibrotic potential and may be the drivers of fibrosis in the IgG4-RD lesions.

Circulating $CD4^+SLAMF7^+$ CTLs diminish in IgG4-RD subjects following rituximab therapy

Therapeutic B-cell depletion with rituximab (an anti-CD20 monoclonal antibody) generally results in clinical improvement in IgG4-RD [42, 43]. $CD19^+$ B cells decline dramatically after rituximab therapy, followed by a clinically apparent reduction in disease activity as measured using the IgG4-RD Responder Index [44]. Interestingly, a significant decrease in the percentages and numbers of $CD4^+SLAMF7^+$ CTLs was also observed up to 12 months after rituximab treatment while the number of naive $CD4^+CD45RA^+$ T cells remained stable (Fig 7, A and B).

Rituximab therapy had minimal or no impact on the frequency and number of $CD4^+GATA\text{-}3^+$ Th2 phenotype cells, or $CD4^+CD25^+Foxp3^+$ T regulatory cells in peripheral blood (Fig 7, C and D). The $CD4^+SLAMF7^+$ CTL numbers decreased despite the fact that these cells do not express any detectable CD20 on their cell surface (Fig E15). In one serially monitored subject, for whom a TCR Vβ-specific antibody was available, rituximab treatment induced a decline in the $V\beta17^+$ CTL clone as well as of total $CD4^+SLAMF7^+$ CTLs (Fig 7, E). A positive clinical response to rituximab therapy was accompanied by a greater than 50% reduction in circulating $CD4^+SLAMF7^+$ CTL numbers (Fig 7, F). These

data provide additional circumstantial evidence for a pathogenic role for IL-1β secreting $CD4^+$ CTLs in IgG4-RD.

Discussion

One of the challenges in human immunology is the difficulty in advancing from correlation to causation. Our studies reveal that a poorly-studied human $CD4^+$ T cell population that secretes pro-fibrotic cytokines is expanded in subjects with IgG4-RD. The demonstration of the clonal expansion of these T cells by next generation sequencing, their localization and in situ re-activation at sites of disease, and their decline following successful therapy provide strong evidence for a likely causal role for IL-1β, IFN-γ and TGF-β1 secreting $CD4^+$ cytotoxic T cells in IgG4-related disease, and likely other fibrotic inflammatory disorders. Such an approach, determining which lymphocytes are clonally expanded and infiltrate tissue sites of disease, may serve as a template for implicating specific adaptive immune cells in disease processes.

This study illustrates several novel and clinically relevant findings. Oligoclonal expansions of circulating $CD4^+SLAMF7^+$ CTLs are seen in IgG4-RD patients, especially during active disease. These T-cell clones are unusual in terms of their ability to make IL-1β, TGF- β1 and IFN-γ; IL-1β is a cytokine typically thought to be produced by non-lymphoid cells [45]. These expanded T cells were also found in affected tissues providing strong evidence for their potential role in disease pathogenesis. The production of large amounts of IL-1β by these T cells following brief re-stimulation, and the expression of pre-formed cytotoxic mediators suggests that the $CD4^+SLAMF7^+$ CTL population represents an unusual and not easily categorized subset of human $CD4^+$ effector T cells that potentially drives the disease process, perhaps in collaboration with other T cells. The secretion of processed IL-1β suggests that inflammasome activation occurs in activated $CD4^+$ CTLs. The mechanism of TGF-β1 induction in $CD4^+$ CTLs and the presumed processing of secreted TGF-β1 in disease tissues remains to be investigated.

Fibrosis is an essential feature of the histopathology of IgG4-RD [46], but the etiology of the fibrosis in this disease has not been clear. IgG4 antibodies are generally considered to be non-inflammatory because they do not efficiently engage activating Fc receptors or complement and may be functionally monovalent in vivo [47]. We have observed active disease in a number of subjects with relatively low levels of plasma IgG4 but a clear expansion of the $CD4^+SLAMF7^+$ CTL population. The contribution of IgG4 antibodies to disease pathogenesis is therefore unclear. It is possible that the IgG4 response seen in disease represents an exaggerated but ineffectual attempt to sequester antigens and dampen inflammation.

Our observations show that clonally-expanded $CD4^+$ CTLs that express granzyme B, perforin, IFN-γ, IL-1β and TGF-β1 are prominent in this disease and a number of prior observations suggest that they may induce the fibrotic pathology seen in IgG4-RD. Transient expression of IL-1β alone in the rat lung has been shown to result in tissue damage and progressive fibrosis [17]. Transgenic overexpression of IL-1β in the murine pancreas results in a fibrotic pancreatitis [18]. IL-1R1/MyD88 signaling and the inflammasome are essential

drivers of the fibrotic process in the widely studied murine model of pulmonary fibrosis induced by bleomycin [16]. IFN-γ has been shown to contribute to fibrosis in a murine thyroiditis model [48]. Indeed IL-1β induced fibrosis in mice has been shown to be dependent on IL-17A and IFN-γ. These $CD4^+$ CTLs observed in IgG4-RD represent an abundant source of IL-1β and TGF-β1 in the tissue lesions of IgG4-RD, thereby potentially driving fibrosis.

In addition to our studies on IgG4-RD, studies on smaller numbers of subjects with systemic sclerosis suggest that $CD4^+Tbet^+SLAMF7^+$ CTLs contribute to the pathogenesis of a broader range of fibrotic inflammatory diseases (Fig E16). The abundance of these cells in subjects with systemic sclerosis, for instance, is similar to that seen in IgG4-RD. $CD4^+CD28^{lo}$ cells, which have been shown to express cytotoxic mediators and IFN-γ in some studies, have previously been identified in idiopathic pulmonary fibrosis, severe rheumatoid arthritis, multiple sclerosis, granulomatosis with polyangiitis (formerly Wegener's granulomatosis) [49–51] and a small proportion of healthy elderly subjects. The $CD4^+SLAMF7^+$ CTLs that we have identified in IgG4-RD subjects also express reduced levels of CD28 and may be related to these previously described $CD4^+CD28^{lo}$ cells. A survey of SLAM family protein expression in systemic lupus erythematosus revealed higher levels of SLAMF7 in some B and T cells, but the cell phenotypes were not characterized further [52].

Many types of fibrosis including murine models of schistosomiasis and bleomycin-induced pulmonary fibrosis have been linked to T_H2 cells and T_H2 cytokines [19]. Although T_H2 cells have been implicated in IgG4-RD in some studies [7–9], we have recently demonstrated that T_H2 cell expansions are highly correlated with the allergic history of patients. We have not seen a consistent expansion of T_H2 effector cells in active IgG4-RD. Instead, we find that IgG4-RD subjects with chronic allergies in addition to fibrotic tumescent lesions have an expansion of both T_H2 cells as well as IL-1β producing $CD4^+$ CTLs and clonal expansions of Th2 cells are not seen even in subjects with concomitant allergic disease (Mattoo et al. submitted; accompanying manuscript). $CD4^+$ CTLs in IgG4-RD subjects synthesize IL-1β and TGF-β1 in affected fibrotic tissues, suggesting that fibrotic disease mechanisms that have been elucidated downstream of IL-1β [30] and TGF-β1 [3] are likely of importance in IgG4-RD.

We have recently demonstrated marked expansions of $IgG4^+$ plasmablasts in IgG4-RD subjects with active disease [53]. Since these plasmablasts express high levels of MHC class II molecules, are depleted by rituximab, and are also present in disease lesions, it is possible that they play an important role in the reactivation of the $CD4^+$CTLs and induce them to either make cytokines including IL-1β and TGFβ1, or to kill parenchymal cells.

The selective decline in $CD4^+$ CTLs, including the expanded clones after rituximab-mediated B-cell depletion, may have broad relevance. These observations imply that in humans, as in rodents, B cells play an important role in the maintenance of effector/memory $CD4^+$ T cells, including disease-associated, "rogue" T-cell clones [54, 55]. These findings may explain why rituximab is effective in diseases such as relapsing-remitting multiple sclerosis in which end-organ damage is primarily mediated by autoreactive T cells. B cells that have the unique ability to bind specific auto-antigens can act as potent antigen-presenting cells at

low antigen concentrations [56], and may provide efficient access to T-cell epitopes. Thus, it is possible that in T-cell mediated autoimmune disorders that are responsive to rituximab therapy, the effector/memory $CD4^+$ T cell response is maintained by B cells. Alternatively, pathogenic T cells may be dependent upon B cell derived growth factors [54]. These possibilities are not mutually exclusive.

The SLAM family is a subset of the immunoglobulin superfamily of receptors. Members of the SLAM family can be involved in both homotypic as well as heterotypic interactions [57, 58]. Given the presence of immune-receptor tyrosine based switch motifs (ITSMs) in its cytoplasmic tail, SLAMF7 can lead to activating or inhibitory signaling within the cell, depending on its association with a SLAM associated protein (SAP) family adaptor called EAT2. Both plasmablasts and $CD4^+$ CTLs in diseased tissue express SLAMF7, and it is unclear at this time whether SLAMF7 in $CD4^+$ CTLs participates in homotypic or heterotypic interactions, or whether it transduces activating or inhibitory signals in these cells.

From a therapeutic standpoint, depleting SLAMF7-expressing cells as well as neutralizing IL-1β may represent rational strategies in a range of immune-mediated conditions associated with severe tissue damage and fibrosis. A few biologic agents that target SLAMF7 or IL-1β are already in clinical use or in advanced stages of drug development. A humanized monoclonal antibody directed against the human SLAMF7, elotuzumab has shown promise in patients with advanced multiple myeloma [59]. Anakinra, a non-glycosylated recombinant form of the naturally occurring IL-1 receptor antagonist that blocks inflammasome dependent IL-1β signaling has been successfully used in type 2 diabetes, asbestosis and other conditions [60]. Canakinumab is a monoclonal antibody that binds to and antagonizes IL-1β and is being studied in a number of clinical trials [61].

In summary, our studies suggest that $CD4^+$ CTLs with a unique hitherto undescribed phenotype expand clonally in the circulation and tissue sites and probably mediate the pathological changes seen in IgG4-RD. These cells elaborate a unique combination of cytokines, some of which are known to contribute to fibrosis in animal models, and the numbers of these cells correlate well with clinical disease activity. Furthermore, therapeutic improvement in IgG4-RD mediated by B cell depletion is linked to a specific reduction of these $CD4^+$ CTLs and not of naive T cells, regulatory T cells or memory T follicular helper cells. Examining subjects with newly diagnosed, untreated and active disease has allowed the identification and characterization of clonally expanded effector T cells linked to disease and to the observation of their attenuation by rituximab. These studies suggest a mechanism by which rituximab mediates clinical improvement in inflammatory disorders that are primarily linked to T cells. Based on our studies, we believe that B cell depletion will also likely prove effective in other immune-mediated disorders involving pathogenic effector T cell subsets that depend upon B cells for antigen presentation or maintenance.

Rituximab infusion of IgG4-RD patients

This study was approved by the institutional review board and informed, written consent was obtained from all subjects referred to or presenting at the rheumatology clinic of the

Massachusetts General Hospital. Twelve IgG4-RD patients with active disease were treated with two 1000 mg doses of rituximab, 15 days apart. 15 mL of peripheral blood was collected at initial presentation and each subsequent clinical visit. These patients were longitudinally followed for 9–15 months at the rheumatology clinic. Peripheral blood was collected in EDTA or ACD tubes (BD Vacutainer) and transported to the laboratory for cell isolation on the same day.

Isolation of mononuclear cells

Mononuclear cells were isolated from peripheral blood of IgG4-RD subjects and healthy controls by Ficoll-Paque Plus (GE Healthcare) density-gradient centrifugation following the manufacturer's protocol. To facilitate subsequent analysis of cells in batches, PBMCs were resuspended in fetal bovine serum containing 10% dimethyl sulfoxide and cryopreserved in vapor phase liquid nitrogen.

Immunofluorescence

Anti-human TCRVβ17-PE (clone E17.5F3.15.13, Beckman-Coulter), anti-human CD4-biotin and mouse anti-biotin Alexa fluor 647 (Life technologies), mouse anti-human CD319 (clone 162.1, Biolegend) and goat anti-mouse Alexa fluor 488 (Life technologies), rabbit polyclonal anti-human IL-1β (Clone 3553, Biovision) and goat anti-rabbit Alexa fluor 488 (Life technologies) were used for immunofluorescence detection of $CD4^+SLAMF7^+$ cells and IL-1β producing $CD4^+$ cells in deparaffinized sections of tissue biopsies using established protocols.

In addition, three multi-color immunofluorescence staining panels CD4/SLAMF7/GATA-3, CD4/SLAMF7/IL-1β and CD4/ TGFβ1 were devised to measure the frequency and in vivo function $CD4^+SLAMF7^+$ CTLs. Detection was performed using mouse or rabbit Superpicture polymer detection kits (HRP; Life Technologies) followed by tyramide signal amplification by Opal 3-plex kit (Perkin Elmer) by following the manufacturer's protocol. The slides were counterstained with DAPI (Thermo Scientific) and mounted using Vectashield mounting medium (Vector labs). Stained tissues were scanned on TissueFAX (Tissuegnostics) and the frequency for $CD4^+$ cells co-expressing SLAMF7 and IL-1β was calculated using the proprietary TissueQuest software. The anti-IL-1β antibody used recognizes primarily the processed mature form of IL-1β.

Flow cytometric analysis

Fluorescence labeling for flow cytometry was performed by incubating cells in staining buffer (Biolegend) containing optimized concentrations of fluorochrome-conjugated antibodies. Except where indicated, all antibodies were procured from Biolegend. The following monoclonal antibodies were used in this study: anti-human CD19-Pacific Blue (clone HIB19), anti-human CD27-APC (clone O323), anti-human CD38-FITC (clone HIT2), anti-human IgG4 (clone 6025, Southern Biotech), anti-human CD4-PE-Cy7 (clone OKT4), anti-human CD8α-PE, anti-human CXCR5-PE (clone J252D4), CD39 (Clone A1), anti-human CD45RA-PE (clone HI100), anti-human CD45RO-APC (clone UCHL1), anti-human CD62L-FITC (clone DREG56), anti-human CD244-biotin (clone C1.7, eBioscience), anti-human CD20-APC, anti-human CD319 (SLAMF7)-PE (clone 162.1),

anti-human CD11b-APC Cy7 (clone ICRF44), anti-human CD28-PerCP Cy5.5 (clone CD28.2), anti-human TCR Vβ23 FITC (clone αHUT7), anti-human TCR Vβ17-PE (clone E17.5F3.15.13, Beckman-Coulter), anti-human TCR Vβ2-PE (clone MPB2D5, Beckman-Coulter), CD39-PE Cy7 (Clone A1, Biolegend) and CD25-APC Cy7 (Clone BC96, Biolegend). A table of concordance between the TCR Vβ gene nomenclatures and IMGT gene names, which is available on the IMGT website (http://www.imgt.org), was used to verify that the appropriate Vβ-specific antibody clones were selected to detect clonally-expanded T-cell clones identified by next-generation sequencing [56].

PBMCs and single cell suspensions from tissue biopsies were reacted with Fc blocking agent (Human FcX, Biolegend). Surface staining was performed using appropriate dilution of antibodies in 12x75mm round bottomed polystyrene tubes in the dark at 4°C. For intracellular staining (T-bet, GATA-3, Foxp3, granzyme B and perforin) cells were fixed and permeabilized with the Foxp3-staining kit (eBioscience) according to manufacturer's guidelines. Cells were then stained in permeabilization buffer with anti-human T-bet PECy7 (clone 4B10, eBioscience), GATA-3 PE-Cy7 (clone L50-823, BD Biosciences), anti-human FOXP3 Alexa Fluor 488 (Clone 206D, Biolegend), anti-human Perforin PE (clone B-D48) and anti-human granzyme B FITC (clone GB11). For the degranulation assay, $CD4^+SLAMF7^+$ CTLs were stimulated with 3 μg/mL anti-human CD3 (OKT3) for 4 hours and surface staining for anti-human CD107a (Biolegend) was performed followed by permeabilization and intra-cellular staining for Granzyme B as discussed above.

EBV-transformed B cell lines from an IgG4-RD patient (P46) were used as targets in the allogeneic CTL assay. 5 x 10^4 EBV-transformed B cells were co-cultured for 12 hours with $CD4^+$ CTLs from two patients at different ratios in presence or absence of anti-CD3. Cells were harvested and surface stained for anti-human CD4 as described above followed by staining with Annexin V-APC in Annexin V binding buffer (15 minutes at room temperature). DAPI was added to the cells at a final concentration of 1 μg/ml. Target cells were gated as CD3-negative and percentage of apoptotic/dead cells were estimated by Annexin $V^+/DAPI^+$ gates.

Intracellular staining for cytokines in restimulated T cells

For detecting intracellular levels of cytokines, mononuclear cells were stimulated with 100 ng/mL of phorbol-myristoyl acetate (Sigma-Aldrich) and 100 ng/mL of ionomycin (Invitrogen) in the presence of Brefeldin A (Sigma-Aldrich) for 4 hrs at 37°C. They were subsequently labeled with the LIVE/DEAD* fixable violet viability dye (Invitrogen) in phosphate-buffered saline for 20 minutes and stained for cell surface markers. Cells were then fixed/permeabilized and stained with anti-human IFN-γ APC (clone 4S.B3), anti-human IL-4 Alexa Fluor® 488 (clone 8D4-8) for 45 minutes on ice. Cells were washed two times with permeabilization buffer and once with PBS and acquired/analyzed on a BD LSR II (BD Biosciences). The .fcs files were analyzed using FlowJo software (version 9.6.3, Treestar).

Cell sorting

To preserve cell viability mononuclear cells were stained with relevant cell surface markers in DMEM (Gibco) with ITS+ Universal Culture Supplement (BD Biosciences). For batch sorts, antibody-stained cells were resuspended at ~20 million/mL in HBSS (Gibco) plus 10 mM glucose and sorted on a BD FACSAria II (BD Biosciences). Sorted cells were collected in 5 mL tubes containing 1 mL collection medium (DMEM with 30% FBS) and re-analyzed on the sorter to ensure > 99% purity in defined gates.

Deep sequencing analysis of TCR Vβ repertoire

Next-generation sequencing analysis of the TCR Vβ repertoire was undertaken using the ImmunoSeq® platform at Adaptive Biotechnologies Inc. at the “survey” level of sequencing depth, that is designed to target an output of 200,000 assembled output sequences after preprocessing filters [57, 58]. Briefly, genomic DNA was isolated from flow-sorted $CD4^+$ T cell subsets (T_{EM}, $CD4^+SLAMF7^+$ CTLs and GATA-3+ T_H2 cells) from individual IgG4-RD subjects. Sorted cell numbers ranged from ~5,000 to ~40,000, assuring at least 5-fold depth of sequencing. Genomic rearrangements of V-D-J gene segments at the TCRβ locus were amplified using multiplex PCR with forward and reverse primers specific for Vβ and Jβ gene segments respectively, and analyzed by paired-end Illumina sequencing. Use of barcoded primers allowed multiplexing of next-generation sequencing samples on an Illumina Hi-Seq instrument. The sequences were assembled in silico, and V-D-J regions were reconstructed, following standard IMGT gene nomenclature for TCR Vβ gene segments [56]. Non-productive rearrangements were excluded from the analysis.

Gene-expression analysis

The nCounter® human immunology panel (NanoString Technologies), comprising ~500 immunology-related genes was used to quantify the gene expression of effector/memory T cells in IgG4-RD. RNA was extracted from 10,000–50,000 flow-sorted T cells using the Qiagen RNAEasy Micro kit according to manufacturer's protocol. Targets were reverse-transcribed and pre-amplified for 14 cycles using the standard multiplexed target enrichment (MTE) protocol (NanoString Technologies) for 458 target genes, which has been previously validated to yield a linear response. The amplified products were hybridized in solution to color-coded nCounter capture and reporter probes and captured on an nCounter Cartridge for high-resolution digital scanning and analysis on the GEN2 Digital Analyzer at NanoString Technologies. The raw gene expression data was normalized to the mean of the spiked-in internal positive control probes to correct for technical assay variation and subsequently normalized to the mean of 15 housekeeping genes included in the nCounter codeset to correct for differences in sample input or variation in reverse-transcription/pre-amplification. Biological replicates were evaluated for consistency and differential expression analysis of gene expression was undertaken using the ComparativeMarkerSelection module in the GenePattern pipeline (version 3.5.0) [59, 60].

Quantitative real time PCR

Total RNA was extracted from ~10,000 – 40,000 cells using the RNAeasy plus Micro kit (Qiagen). cDNA was synthesized using a RT2 first-strand kit (Qiagen) followed by

quantitative real time PCR analysis (SYBR green; Life technologies). GAPDH mRNA expression was used as the normalizing control. The primers used were:

ThPOK (F: 5'-gtctgccacaagatcatcca-3', R: 5'-tcgtagctgtgcaggaagc-3'),

Runx3 (F:5'cagaagctggaggaccagac-3', R: 5'-gtcggagaatgggttcagtt-3') &

GAPDH (F: 5'-atgttcgtcatgggtgtgaa-3', R: 5'-gtcttctgggtggcagtgat-3')

ELISpot and western blotting for IL-1β

Prior to coating, 96-well polyvinylidene difluoride (PVDF) membrane plates (Millipore) were prewet with 50ul 70% ethanol/well for 2 minutes and washed three times with 200ul sterile filtered water. ELISpot assay for IL-1β was performed using human IL-1β ELISpot Ready-SET-Go kit (eBioscience) according to the manufacturer's recommendations. In brief, plates were coated overnight at 4°C with the anti-human IL-1β antibody provided, followed by gentle washing with ELISpot wash buffer (1X PBS plus 0.05% Tween-20) and blocking with complete medium (RPMI plus 10% fetal bovine serum) for 2 hours at room temperature. 10000 sorted $CD4^+CD45RO^+$ cells from healthy controls and IgG4-RD patients were rested on the plate in complete medium for 4 hours post-sorting, and stimulated with PMA (100ng/ml) and ionomycin (100ng/ml) overnight at 37°C. Cells were decanted gently using wash buffer to detach any adherent cells and plates were washed three times with wash buffer followed by incubation with the recommended dilution of biotinylated detection antibody for 2 hours at room temperature. After two additional washes, plates were incubated with horse-radish peroxidase conjugated with streptavidin for 45 minutes at room temperature. The plates were washed extensively 4 times with wash buffer followed by two additional washes with PBS to remove any traces of tween-20. 100 μL of TMB substrate (MabTech) was added and spots were allowed to develop for upto 20 minutes. Counting and visual analysis of the spots were done using a computer-operated CTL ELISpot reader and the fraction of IL-1β secreting cells was quantified as the number of spots detected per 10,000 cells applied to the well.

For Western blot analysis of secreted IL-1β, $CD4^+CD45RO^+$ cells from healthy donors, $CD4^+CD27^-$ gated $SLAMF7^+$ and $SLAMF7^-$ cells from an IgG4-RD subject were sorted and expanded in vitro in a U-bottomed 96-well plate (BD Falcon) with weekly anti-CD3 stimulation (Biolegend; OKT3, 3μg/ml) in media supplemented with 10ng/mL of rhIL-2. 150,000 cells were re-stimulated with anti-human CD3 (Biolegend; OKT3, 3μg/ml) or Lipopolysaccharide (LPS; Sigma, 5μg/ml) and the culture supernatants were harvested at 60hrs. These supernatants were run on an SDS-PAGE gel and transferred onto Immobilon-P membranes. IL-1β was detected using a rabbit anti-human IL-1β antibody (Biovision) followed by goat anti-rabbit Ig-HRP (Thermo scientific) and developed using SuperSignal West Pico Chemiluminescent Substrate (Biorad). LPS stimulated PBMCs were used as positive controls.

ELISA for TGFβ1

$CD4^+$ CTLs and $CD4^+CD45RA^+$ naïve cells from IgG4-RD patients were stimulated in vitro in 96 well plates (50,000 cells/well) with anti-human CD3 (Biolegend; OKT3, 3μg/ml) in media supplemented with 10ng/mL of rhIL-2 and the culture supernatants were harvested

at 48hrs. ELISA was performed on these culture supernatants using a Human TGFβ1 Quantikine ELISA kit using the manufacturer's protocol. Standards provided in the kit were used to quantify TGFβ1 in culture supernatants.

Supplementary Material

Refer to Web version on PubMed Central for supplementary material.

Acknowledgments

This study was funded by grants U19-AI110495 and AI 113163 from the NIH. The MGH flow core is supported by grant S10RR023440 from the NIH.

Abbreviations

IgG4-RD	IgG4 related disease
CD4$^+$ CTL	CD4$^+$ cytotoxic T lymphocyte
ECM	Extra-cellular matrix
IgG4-DS	IgG4-related dacryoadenitis and sialadenitis
SS	Sjögren's syndrome
ANA	Anti-nuclear antibodies
PBMCs	Peripheral blood mono-nuclear cells
TCR	T-cell receptor
PMA	Phorbol 12-myristate 13-acetate
LPS	Lipo-polysaccharide
ELISPOT	Enzyme-Linked ImmunoSpot

References

1. Stone JH, Zen Y, Deshpande V. IgG4-related disease. N Engl J Med. 2012; 366:539–51. [PubMed: 22316447]
2. Mahajan VS, Mattoo H, Deshpande V, Pillai SS, Stone JH. IgG4-Related Disease. Annu Rev Pathol. 2014; 9:315–47. [PubMed: 24111912]
3. Kamisawa T, Zen Y, Pillai S, Stone JH. IgG4-related disease. Lancet. 2015; 385:1460–71. [PubMed: 25481618]
4. Bindon CI, Hale G, Bruggemann M, Waldmann H. Human monoclonal IgG isotypes differ in complement activating function at the level of C4 as well as C1q. J Exp Med. 1988; 168:127–42. [PubMed: 3260935]
5. Bruhns P, Iannascoli B, England P, Mancardi DA, Fernandez N, Jorieux S, et al. Specificity and affinity of human Fcgamma receptors and their polymorphic variants for human IgG subclasses. Blood. 2009; 113:3716–25. [PubMed: 19018092]
6. Aoki S, Nakazawa T, Ohara H, Sano H, Nakao H, Joh T, et al. Immunohistochemical study of autoimmune pancreatitis using anti-IgG4 antibody and patients' sera. Histopathology. 2005; 47:147–58. [PubMed: 16045775]

7. Tanaka A, Moriyama M, Nakashima H, Miyake K, Hayashida JN, Maehara T, et al. Th2 and regulatory immune reactions contribute to IgG4 production and the initiation of Mikulicz disease. Arthritis Rheum. 2012; 64:254–63. [PubMed: 21898360]
8. Kanari H, Kagami S, Kashiwakuma D, Oya Y, Furuta S, Ikeda K, et al. Role of Th2 cells in IgG4-related lacrimal gland enlargement. Int Arch Allergy Immunol. 2010; 152(Suppl 1):47–53. [PubMed: 20523063]
9. Zen Y, Fujii T, Harada K, Kawano M, Yamada K, Takahira M, et al. Th2 and regulatory immune reactions are increased in immunoglobin G4-related sclerosing pancreatitis and cholangitis. Hepatology. 2007; 45:1538–46. [PubMed: 17518371]
10. Okazaki K, Uchida K, Ohana M, Nakase H, Uose S, Inai M, et al. Autoimmune-related pancreatitis is associated with autoantibodies and a Th1/Th2-type cellular immune response. Gastroenterology. 2000; 118:573–81. [PubMed: 10702209]
11. Johnson S, Eller M, Teigler JE, Maloveste SM, Schultz BT, Soghoian DZ, et al. Cooperativity of HIV-Specific Cytolytic CD4 T Cells and CD8 T Cells in Control of HIV Viremia. J Virol. 2015; 89:7494–505. [PubMed: 25972560]
12. Della Torre E, Mattoo H, Mahajan VS, Carruthers M, Pillai S, Stone JH. Prevalence of atopy, eosinophilia, and IgE elevation in IgG4-related disease. Allergy. 2014; 69:269–72. [PubMed: 24266692]
13. Mattoo H, Della-Torre E, Mahajan VS, Stone JH, Pillai S. Circulating Th2 memory cells in IgG4-related disease are restricted to a defined subset of subjects with atopy. Allergy. 2014; 69:399–402. [PubMed: 24382311]
14. Wick G, Backovic A, Rabensteiner E, Plank N, Schwentner C, Sgonc R. The immunology of fibrosis: innate and adaptive responses. Trends Immunol. 2010; 31:110–9. [PubMed: 20106721]
15. Wynn TA, Ramalingam TR. Mechanisms of fibrosis: therapeutic translation for fibrotic disease. Nat Med. 2012; 18:1028–40. [PubMed: 22772564]
16. Gasse P, Mary C, Guenon I, Noulin N, Charron S, Schnyder-Candrian S, et al. IL-1R1/MyD88 signaling and the inflammasome are essential in pulmonary inflammation and fibrosis in mice. J Clin Invest. 2007; 117:3786–99. [PubMed: 17992263]
17. Kolb M, Margetts PJ, Anthony DC, Pitossi F, Gauldie J. Transient expression of IL-1beta induces acute lung injury and chronic repair leading to pulmonary fibrosis. J Clin Invest. 2001; 107:1529–36. [PubMed: 11413160]
18. Marrache F, Tu SP, Bhagat G, Pendyala S, Osterreicher CH, Gordon S, et al. Overexpression of interleukin-1beta in the murine pancreas results in chronic pancreatitis. Gastroenterology. 2008; 135:1277–87. [PubMed: 18789941]
19. Wynn TA. Fibrotic disease and the T(H)1/T(H)2 paradigm. Nat Rev Immunol. 2004; 4:583–94. [PubMed: 15286725]
20. Doucet C, Brouty-Boye D, Pottin-Clemenceau C, Canonica GW, Jasmin C, Azzarone B. Interleukin (IL) 4 and IL-13 act on human lung fibroblasts. Implication in asthma. J Clin Invest. 1998; 101:2129–39. [PubMed: 9593769]
21. Sempowski GD, Beckmann MP, Derdak S, Phipps RP. Subsets of murine lung fibroblasts express membrane-bound and soluble IL-4 receptors. Role of IL-4 in enhancing fibroblast proliferation and collagen synthesis. J Immunol. 1994; 152:3606–14. [PubMed: 7908305]
22. Fuschiotti P. Role of IL-13 in systemic sclerosis. Cytokine. 2011; 56:544–9. [PubMed: 21920770]
23. Kolodsick JE, Toews GB, Jakubzick C, Hogaboam C, Moore TA, McKenzie A, et al. Protection from fluorescein isothiocyanate-induced fibrosis in IL-13-deficient, but not IL-4-deficient, mice results from impaired collagen synthesis by fibroblasts. J Immunol. 2004; 172:4068–76. [PubMed: 15034018]
24. Lee CG, Homer RJ, Zhu Z, Lanone S, Wang X, Koteliansky V, et al. Interleukin-13 induces tissue fibrosis by selectively stimulating and activating transforming growth factor beta(1). J Exp Med. 2001; 194:809–21. [PubMed: 11560996]
25. Murray LA, Argentieri RL, Farrell FX, Bracht M, Sheng H, Whitaker B, et al. Hyper-responsiveness of IPF/UIP fibroblasts: interplay between TGFbeta1, IL-13 and CCL2. Int J Biochem Cell Biol. 2008; 40:2174–82. [PubMed: 18395486]

26. Oh MH, Oh SY, Yu J, Myers AC, Leonard WJ, Liu YJ, et al. IL-13 induces skin fibrosis in atopic dermatitis by thymic stromal lymphopoietin. J Immunol. 2011; 186:7232–42. [PubMed: 21576506]
27. Weng HL, Liu Y, Chen JL, Huang T, Xu LJ, Godoy P, et al. The etiology of liver damage imparts cytokines transforming growth factor beta1 or interleukin-13 as driving forces in fibrogenesis. Hepatology. 2009; 50:230–43. [PubMed: 19441105]
28. Wynn TA, Barron L. Macrophages: master regulators of inflammation and fibrosis. Semin Liver Dis. 2010; 30:245–57. [PubMed: 20665377]
29. Deshpande V. The pathology of IgG4-related disease: critical issues and challenges. Semin Diagn Pathol. 2012; 29:191–6. [PubMed: 23068297]
30. Johansson SG, Hourihane JO, Bousquet J, Bruijnzeel-Koomen C, Dreborg S, Haahtela T, et al. A revised nomenclature for allergy. An EAACI position statement from the EAACI nomenclature task force. Allergy. 2001; 56:813–24. [PubMed: 11551246]
31. Larimore K, McCormick MW, Robins HS, Greenberg PD. Shaping of human germline IgH repertoires revealed by deep sequencing. J Immunol. 2012; 189:3221–30. [PubMed: 22865917]
32. Robins HS, Campregher PV, Srivastava SK, Wacher A, Turtle CJ, Kahsai O, et al. Comprehensive assessment of T-cell receptor beta-chain diversity in alphabeta T cells. Blood. 2009; 114:4099–107. [PubMed: 19706884]
33. Della Torre E, Mattoo H, Mahajan VS, Carruthers M, Pillai S, Stone JH. Prevalence of atopy, eosinophilia, and IgE elevation in IgG4-related disease. Allergy. 2013
34. De Jong R, Brouwer M, Hooibrink B, Van der Pouw-Kraan T, Miedema F, Van Lier RA. The CD27- subset of peripheral blood memory CD4+ lymphocytes contains functionally differentiated T lymphocytes that develop by persistent antigenic stimulation in vivo. Eur J Immunol. 1992; 22:993–9. [PubMed: 1348033]
35. Sallusto F, Lenig D, Forster R, Lipp M, Lanzavecchia A. Two subsets of memory T lymphocytes with distinct homing potentials and effector functions. Nature. 1999; 401:708–12. [PubMed: 10537110]
36. Koyabu M, Uchida K, Miyoshi H, Sakaguchi Y, Fukui T, Ikeda H, et al. Analysis of regulatory T cells and IgG4-positive plasma cells among patients of IgG4-related sclerosing cholangitis and autoimmune liver diseases. J Gastroenterol. 2010; 45:732–41. [PubMed: 20087609]
37. Soghoian DZ, Streeck H. Cytolytic CD4(+) T cells in viral immunity. Expert Rev Vaccines. 2010; 9:1453–63. [PubMed: 21105780]
38. Mucida D, Husain MM, Muroi S, van Wijk F, Shinnakasu R, Naoe Y, et al. Transcriptional reprogramming of mature CD4(+) helper T cells generates distinct MHC class II-restricted cytotoxic T lymphocytes. Nat Immunol. 2013; 14:281–9. [PubMed: 23334788]
39. Stone JH, Khosroshahi A, Hilgenberg A, Spooner A, Isselbacher EM, Stone JR. IgG4-related systemic disease and lymphoplasmacytic aortitis. Arthritis Rheum. 2009; 60:3139–45. [PubMed: 19790067]
40. Della-Torre E, Mattoo H, Mahajan VS, Deshpande V, Krause D, Song P, et al. IgG4-related midline destructive lesion. Ann Rheum Dis. 2014
41. Yamashita M, Ukai-Tadenuma M, Miyamoto T, Sugaya K, Hosokawa H, Hasegawa A, et al. Essential role of GATA3 for the maintenance of type 2 helper T (Th2) cytokine production and chromatin remodeling at the Th2 cytokine gene loci. J Biol Chem. 2004; 279:26983–90. [PubMed: 15087456]
42. Khosroshahi A, Carruthers MN, Deshpande V, Unizony S, Bloch DB, Stone JH. Rituximab for the treatment of IgG4-related disease: lessons from 10 consecutive patients. Medicine (Baltimore). 2012; 91:57–66. [PubMed: 22210556]
43. Khosroshahi A, Bloch DB, Deshpande V, Stone JH. Rituximab therapy leads to rapid decline of serum IgG4 levels and prompt clinical improvement in IgG4-related systemic disease. Arthritis Rheum. 2010; 62:1755–62. [PubMed: 20191576]
44. Carruthers MN, Stone JH, Deshpande V, Khosroshahi A. Development of an IgG4-RD Responder Index. Int J Rheumatol. 2012; 2012:259408. [PubMed: 22611406]
45. Dinarello CA. Immunological and inflammatory functions of the interleukin-1 family. Annu Rev Immunol. 2009; 27:519–50. [PubMed: 19302047]

46. Deshpande V, Zen Y, Chan JK, Yi EE, Sato Y, Yoshino T, et al. Consensus statement on the pathology of IgG4-related disease. Mod Pathol. 2012; 25:1181–92. [PubMed: 22596100]
47. Aalberse RC, Stapel SO, Schuurman J, Rispens T. Immunoglobulin G4: an odd antibody. Clin Exp Allergy. 2009; 39:469–77. [PubMed: 19222496]
48. Chen K, Wei Y, Sharp GC, Braley-Mullen H. Balance of proliferation and cell death between thyrocytes and myofibroblasts regulates thyroid fibrosis in granulomatous experimental autoimmune thyroiditis (G-EAT). J Leukoc Biol. 2005; 77:166–72. [PubMed: 15536125]
49. Martens PB, Goronzy JJ, Schaid D, Weyand CM. Expansion of unusual CD4+ T cells in severe rheumatoid arthritis. Arthritis Rheum. 1997; 40:1106–14. [PubMed: 9182921]
50. Komocsi A, Lamprecht P, Csernok E, Mueller A, Holl-Ulrich K, Seitzer U, et al. Peripheral blood and granuloma CD4(+)CD28(−) T cells are a major source of interferon-gamma and tumor necrosis factor-alpha in Wegener's granulomatosis. Am J Pathol. 2002; 160:1717–24. [PubMed: 12000723]
51. Gilani SR, Vuga LJ, Lindell KO, Gibson KF, Xue J, Kaminski N, et al. CD28 down-regulation on circulating CD4 T-cells is associated with poor prognoses of patients with idiopathic pulmonary fibrosis. PLoS One. 2010; 5:e8959. [PubMed: 20126467]
52. Kim JR, Mathew SO, Patel RK, Pertusi RM, Mathew PA. Altered expression of signalling lymphocyte activation molecule (SLAM) family receptors CS1 (CD319) and 2B4 (CD244) in patients with systemic lupus erythematosus. Clin Exp Immunol. 2010; 160:348–58. [PubMed: 20345977]
53. Mattoo H, Mahajan VS, Della-Torre E, Sekigami Y, Carruthers M, Wallace ZS, et al. De novo oligoclonal expansions of circulating plasmablasts in active and relapsing IgG4-related disease. J Allergy Clin Immunol. 2014 provisionally accepted.
54. Barr TA, Shen P, Brown S, Lampropoulou V, Roch T, Lawrie S, et al. B cell depletion therapy ameliorates autoimmune disease through ablation of IL-6-producing B cells. J Exp Med. 2012; 209:1001–10. [PubMed: 22547654]
55. Crawford A, Macleod M, Schumacher T, Corlett L, Gray D. Primary T cell expansion and differentiation in vivo requires antigen presentation by B cells. J Immunol. 2006; 176:3498–506. [PubMed: 16517718]
56. Rock KL, Benacerraf B, Abbas AK. Antigen presentation by hapten-specific B lymphocytes. I. Role of surface immunoglobulin receptors. J Exp Med. 1984; 160:1102–13. [PubMed: 6207262]
57. Veillette A, Guo H. CS1, a SLAM family receptor involved in immune regulation, is a therapeutic target in multiple myeloma. Crit Rev Oncol Hematol. 2013; 88:168–77. [PubMed: 23731618]
58. De Calisto J, Wang N, Wang G, Yigit B, Engel P, Terhorst C. SAP-Dependent and -Independent Regulation of Innate T Cell Development Involving SLAMF Receptors. Front Immunol. 2014; 5:186. [PubMed: 24795728]
59. Zonder JA, Mohrbacher AF, Singhal S, van Rhee F, Bensinger WI, Ding H, et al. A phase 1, multicenter, open-label, dose escalation study of elotuzumab in patients with advanced multiple myeloma. Blood. 2012; 120:552–9. [PubMed: 22184404]
60. Menu P, Vince JE. The NLRP3 inflammasome in health and disease: the good, the bad and the ugly. Clin Exp Immunol. 2011; 166:1–15. [PubMed: 21762124]
61. Chakraborty A, Tannenbaum S, Rordorf C, Lowe PJ, Floch D, Gram H, et al. Pharmacokinetic and pharmacodynamic properties of canakinumab, a human anti-interleukin-1beta monoclonal antibody. Clin Pharmacokinet. 2012; 51:e1–18. [PubMed: 22550964]

Key messages

- $CD4^+$ T effector memory cells with cytolytic and myeloid features are expanded in IgG4-RD patients.
- $CD4^+SLAMF7^+$ CTLs are clonally expanded while $CD4^+GATA3^+$ T_H2 memory cells in atopic IgG4-RD patients are clonally diverse. $GATA3^+$ T_H2 cells represent a minor proportion of $CD4^+$ cells in affected tissues.
- In IgG4-RD patients $CD4^+SLAMF7^+$ CTLs infiltrate the diseased tissues and secrete the pro-fibrotic cytokines IL-1β and TGF-β1.
- The decline in $CD4^+SLAMF7^+$ CTL numbers upon rituximab therapy is associated with clinical remission of IgG4-RD patients

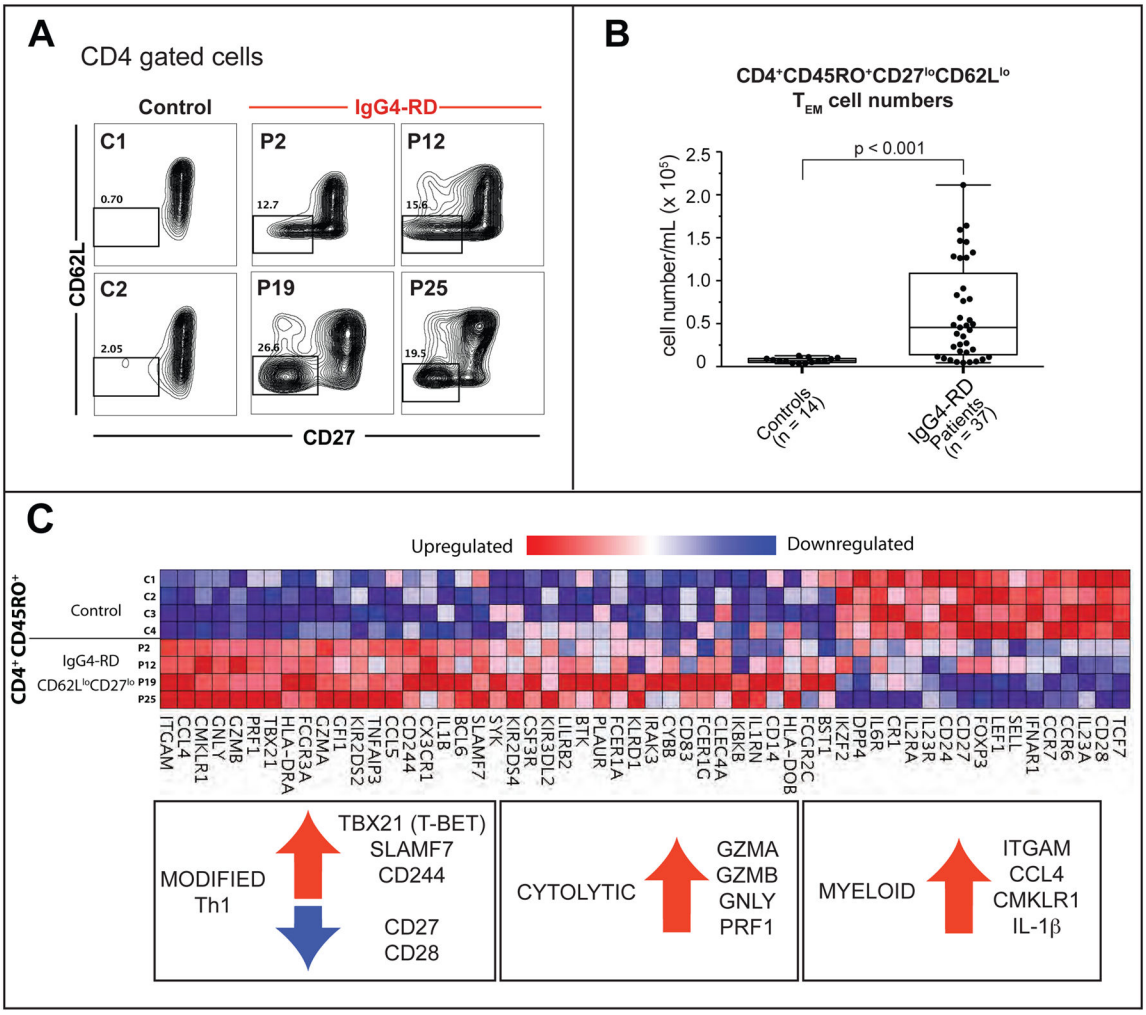

Figure 1. Expansions of T_{EM} cells with a cytolytic phenotype in IgG4-RD

(A) $CD4^+CD62L^{lo}CD27^{lo}$ T_{EM} cells in two non-atopic (P2 & P19) two atopic (P12 & P25) IgG4-RD patients and 2 representative healthy controls.

(B) $CD4^+CD45RO^+CD62L^{lo}CD27^{lo}$ T_{EM} cells in peripheral blood of IgG4-RD subjects. Boxplot displays the 25^{th} to 75^{th} percentiles. P values are based on the Mann-Whitney test.

(C) Heat map depicting differentially expressed immune-related genes in T_{EM} cells from four IgG4-RD patients compared to $CD4^+CD45RO^+$ T cells from four healthy controls. Upregulated genes representing modified Th1, cytolytic and myeloid signatures are highlighted.

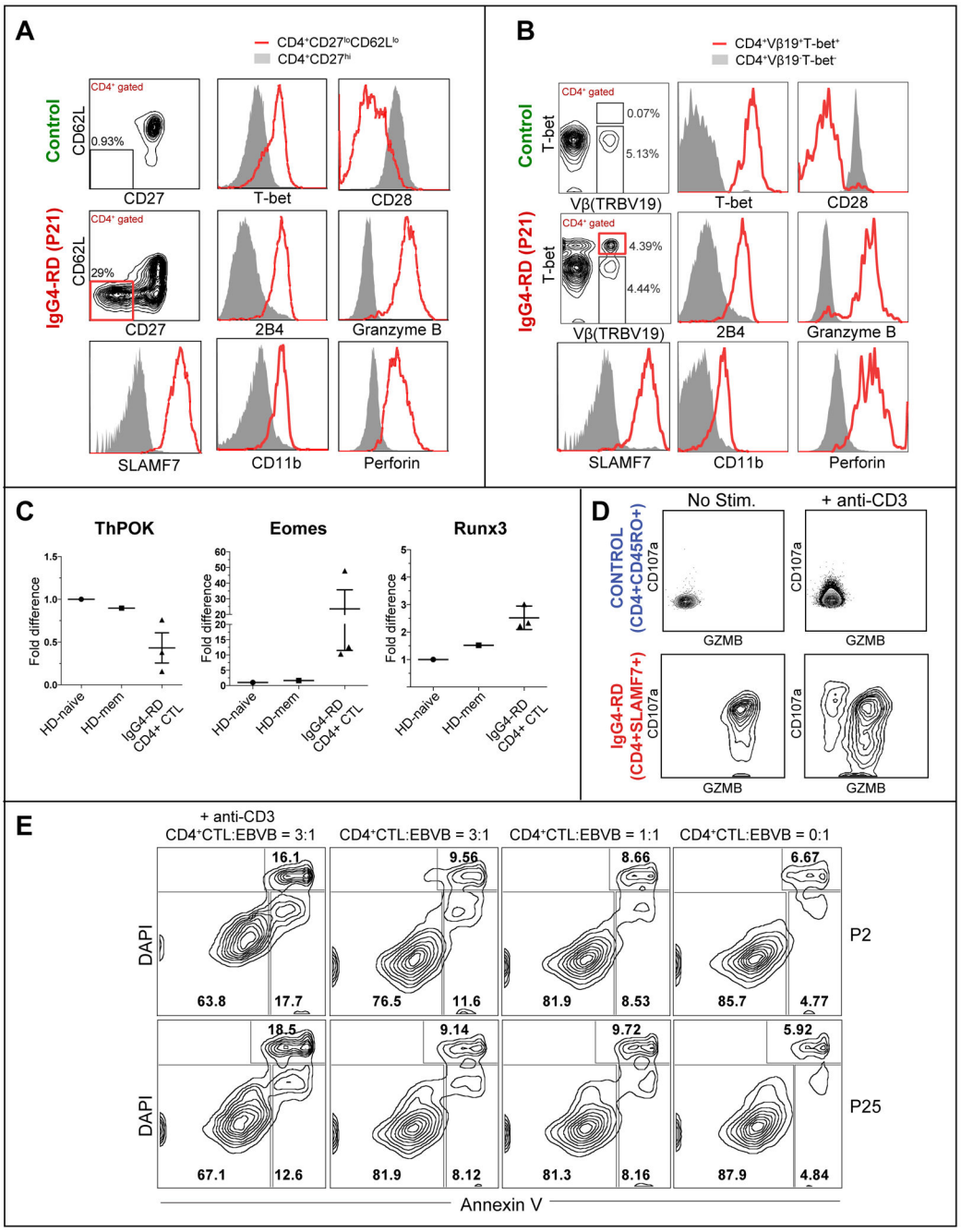

Figure 2. Expanded T_{EM} cells in IgG4-RD subjects exhibit a functional cytolytic profile

(A & B) Key hits from the gene expression analysis from Fig. 1 were validated using flow cytometry in T_{EM} cells (A) and using TCR Vβ-specific antibodies (B).

(C) Levels of ThPOK and Runx3 in $CD4^+SLAMF7^+$ CTLs from IgG4-RD subjects and $CD4^+CD45RO^+$ T cells in healthy controls. Error bars show SEM. P values are based on the Mann-Whitney test.

(D) Granzyme B and CD107a staining on $CD4^+$ CTLs from an IgG4-RD patient, before and after stimulation with anti-CD3 .

(E) Cytotoxicity of in vitro expanded $CD4^+$ CTLs derived from two subjects (P2 and P25) against an allogeneic EBV-transformed B cell target cell line, measured after 12 hours of co-culture with or without anti-CD3 (10 μg/mL) at varying $CD4^+$ CTL: target ratios. The data are representative of two separate experiments done on 4 patients.

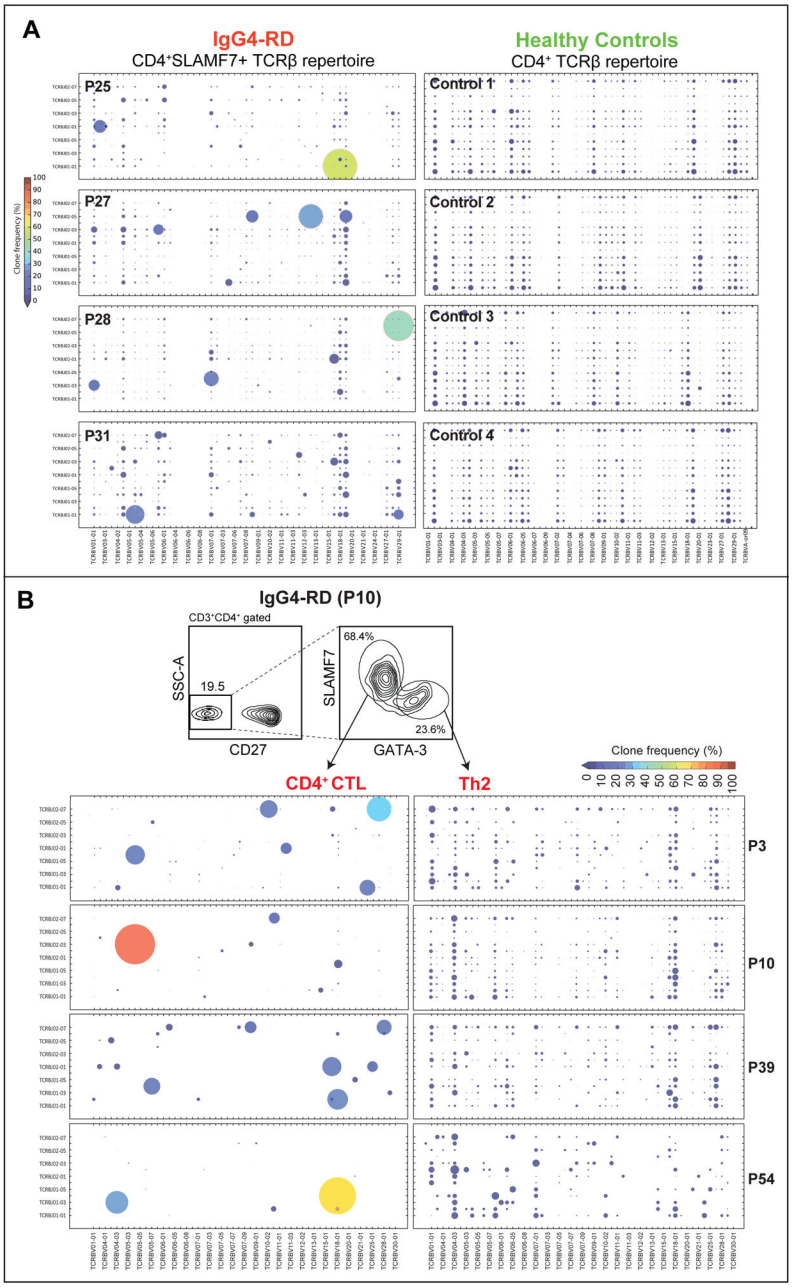

Figure 3. The TCR Vβ repertoire of expanded T_{EM} cells in IgG4-RD

(A) TCRβ repertoire of the expanded circulating T_{EM} subset in 4 IgG4-RD subjects (P31, P28, P27 and P25) and from total CD4+ T cells from four healthy controls, represented as bubble charts, where the size and color corresponds to the frequency of the observed Vβ-Jβ rearrangements.

(B) TCRβ repertoire of expanded circulating $CD4^+GATA\text{-}3^+$ T_H2 cells in four IgG4-RD subjects with an atopic history (P3, P10, P39 & P54), contrasted with the expanded $CD4^+SLAMF7^+$ CTLs from the same individuals. See legend to Fig.3A for details.

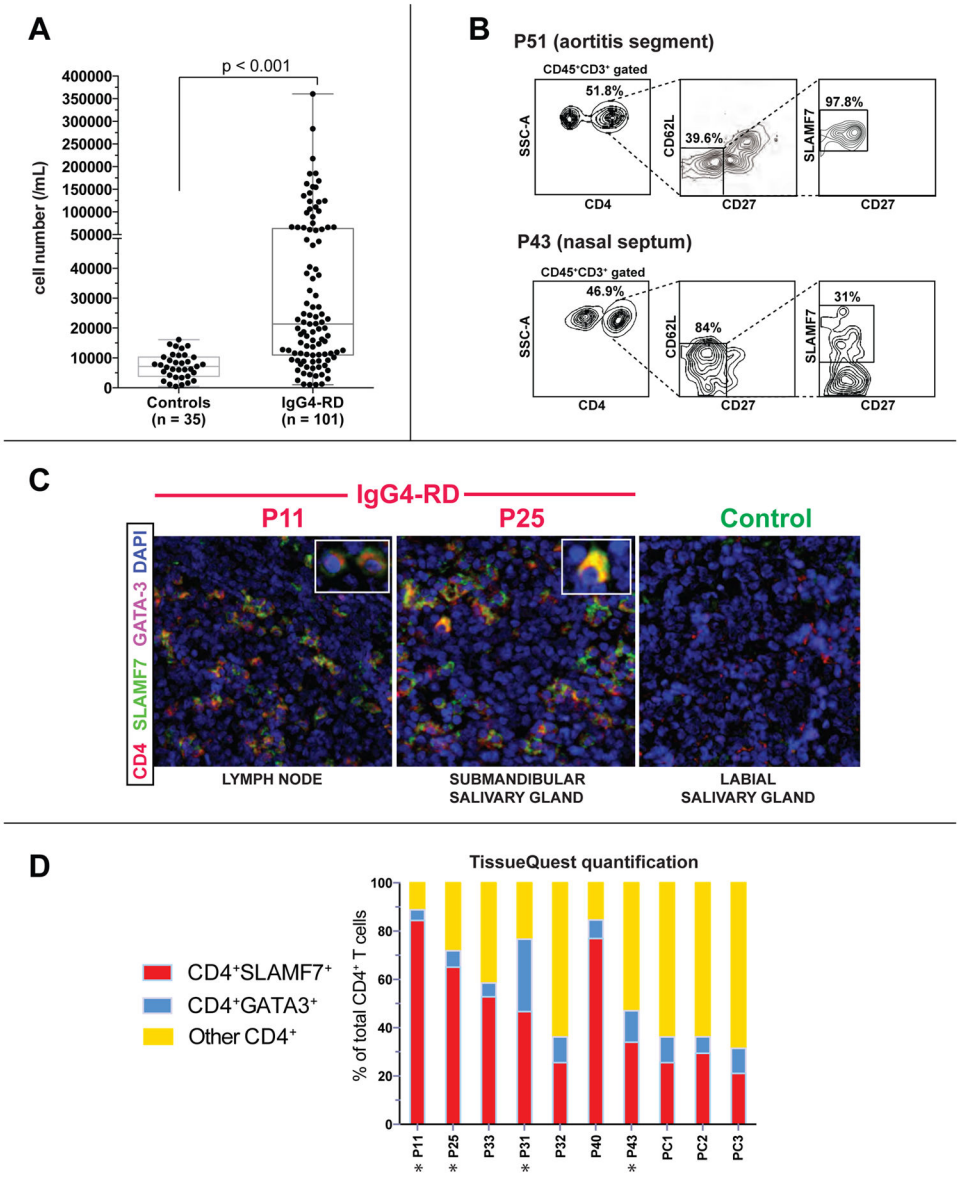

Figure 4. Expansion of CD4$^+$SLAMF7$^+$ CTLs in tissue lesions of IgG4-RD subjects

(A) Expansion of CD4$^+$SLAMF7$^+$ CTLs in 101 IgG4-RD subjects.

(B) CD4$^+$CD62L^{lo}CD27^{lo}SLAMF7$^+$ CTLs in the aortic wall of a subject with IgG4-related aortitis (P51) and the involved nasal septum of a subject with IgG4-RD (P43).

(C) Immunofluorescence staining of CD4+SLAMF7+ CTLs and CD4+GATA-3+ Th2 cells in the affected tissues of IgG4-RD subjects (lymph node biopsy from P11 and salivary gland biopsy from P25). CD4 (red), DAPI (blue), GATA-3 (magenta) and SLAMF7 (green) staining are shown.

(D) Quantification of CD4+SLAMF7+, CD4+GATA-3+ and CD4+SLAMF7-GATA-3- cells in tissue biopsies from 10 IgG4-RD patients (atopic patients are marked with asterisks).

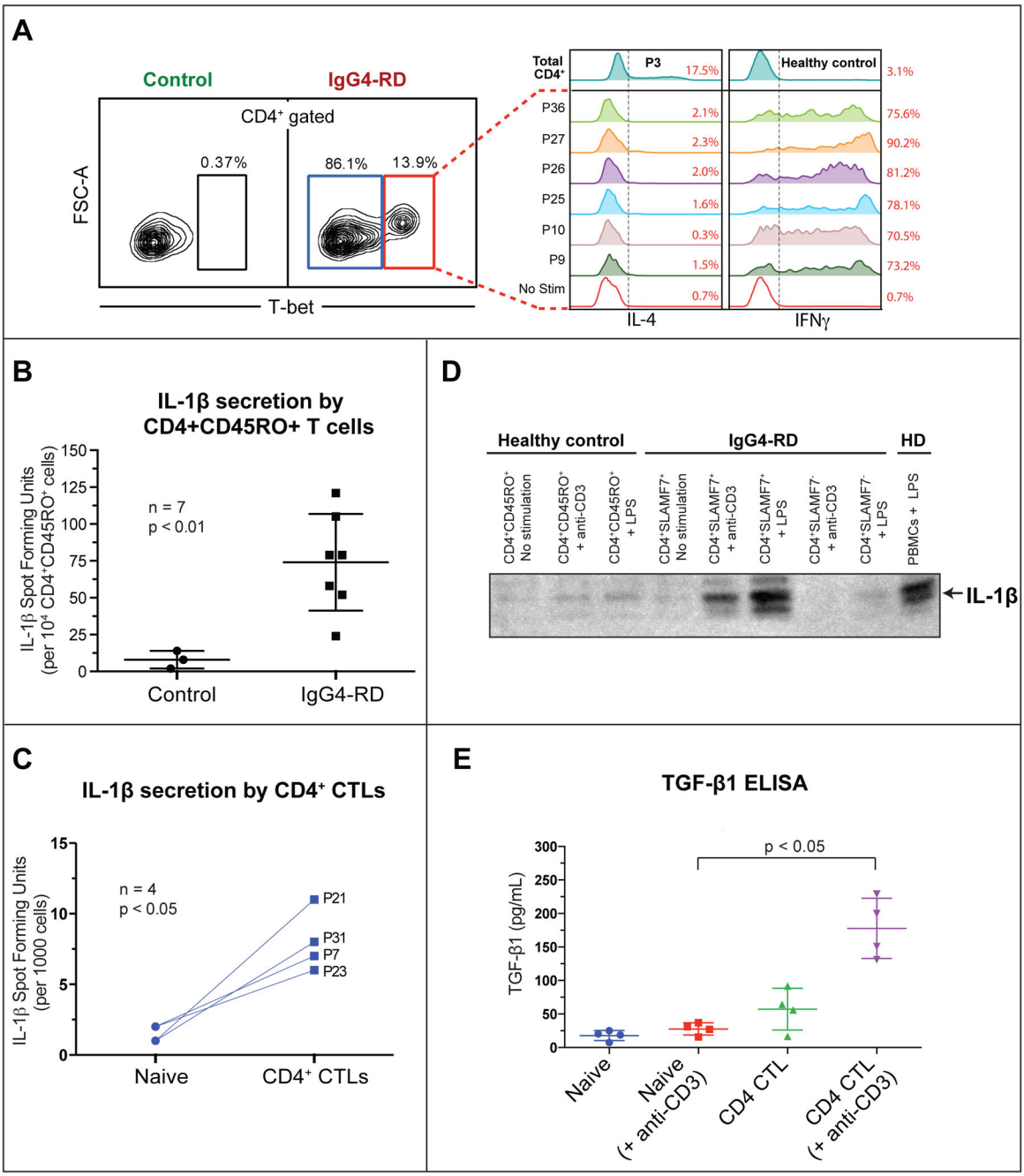

Figure 5. Disease associated CD4⁺ CTLs secrete IFNγ, IL-1β and TGF-β1 upon in vitro restimulation

(A) Intracellular staining for IFN-γ and IL-4 in restimulated CD4⁺ CTLs from seven IgG4-RD patients. The empty histogram (red) depicts an unstimulated control.

(B & C) ELISPOT detection of the frequency of IL-1β producers among re-stimulated CD4⁺CD45RO⁺ T cells from seven IgG4-RD subjects compared to healthy donors (error bars show SEM, unpaired t-test) (A) and CD4⁺ CTLs from four IgG4-RD subjects compared to naïve CD4⁺CD45RA⁺ T cells from the same individuals ($p < 0.05$, paired t-test) (B).

(D) Western Blot detection of IL-1β from culture supernatants of in vitro expanded T cells, maintained in IL-2 for two weeks (10 ng/mL). Supernatants from $CD4^+CD45RO^+$ T cells from a healthy donor and $CD4^+CD45RO^+SLAMF7^+$ or $CD4^+CD45RO^+SLAMF7^-$ T cells from an IgG4-RD subject were used without any stimulation (US), with 5 μg/mL LPS or 3μg/mL anti-CD3. LPS stimulated PBMCs from a healthy donor were used as a positive control.

(E) Detection of TGF-β1 production among naïve $CD4^+$ cells and $CD4^+SLAMF7^+$ CTLs from four IgG4-RD subjects by ELISA, with or without in vitro re-stimulation (with 3 μg/mL anti-CD3). Error bars show SEM. P values are based on the Mann-Whitney test.

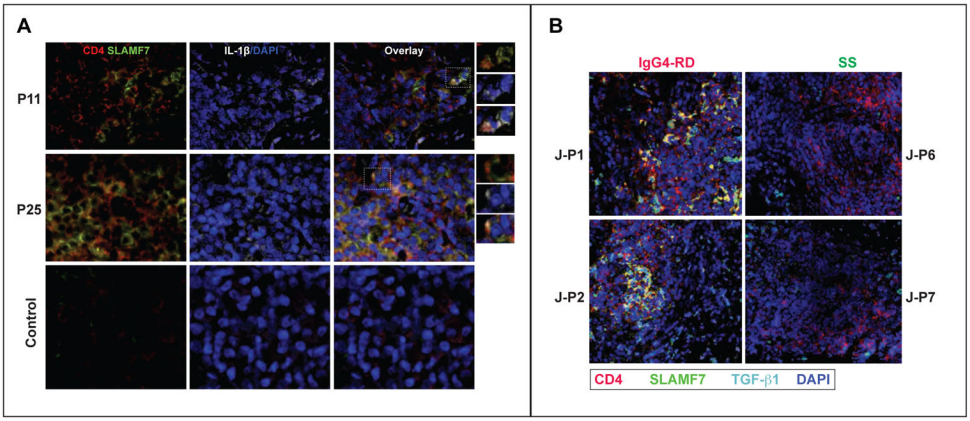

Figure 6. Expansion of IL-1β and TGF-β1 secreting CD4$^+$ CTLs in IgG4-RD lesions

(A) Immunofluorescence staining of IL-1β-producing CD4$^+$ SLAMF7$^+$ cells in the tissues of 2 IgG4-RD subjects (lymph node biopsy from P11 and salivary gland biopsy from P25) and a healthy control subject (labial salivary gland biopsy). CD4 (red), SLAMF7 (green) DAPI (blue) and IL-1β (white).

(B) Immunofluorescence staining of TGF-β1-producing CD4$^+$ SLAMF7$^+$ cells in the tissues of 2 IgG4-DS and 2 Sjögren's syndrome subjects (submandibular salivary gland biopsies). CD4 (red), Granzyme A (green) DAPI (blue) and IL-1β (cyan) staining are shown.

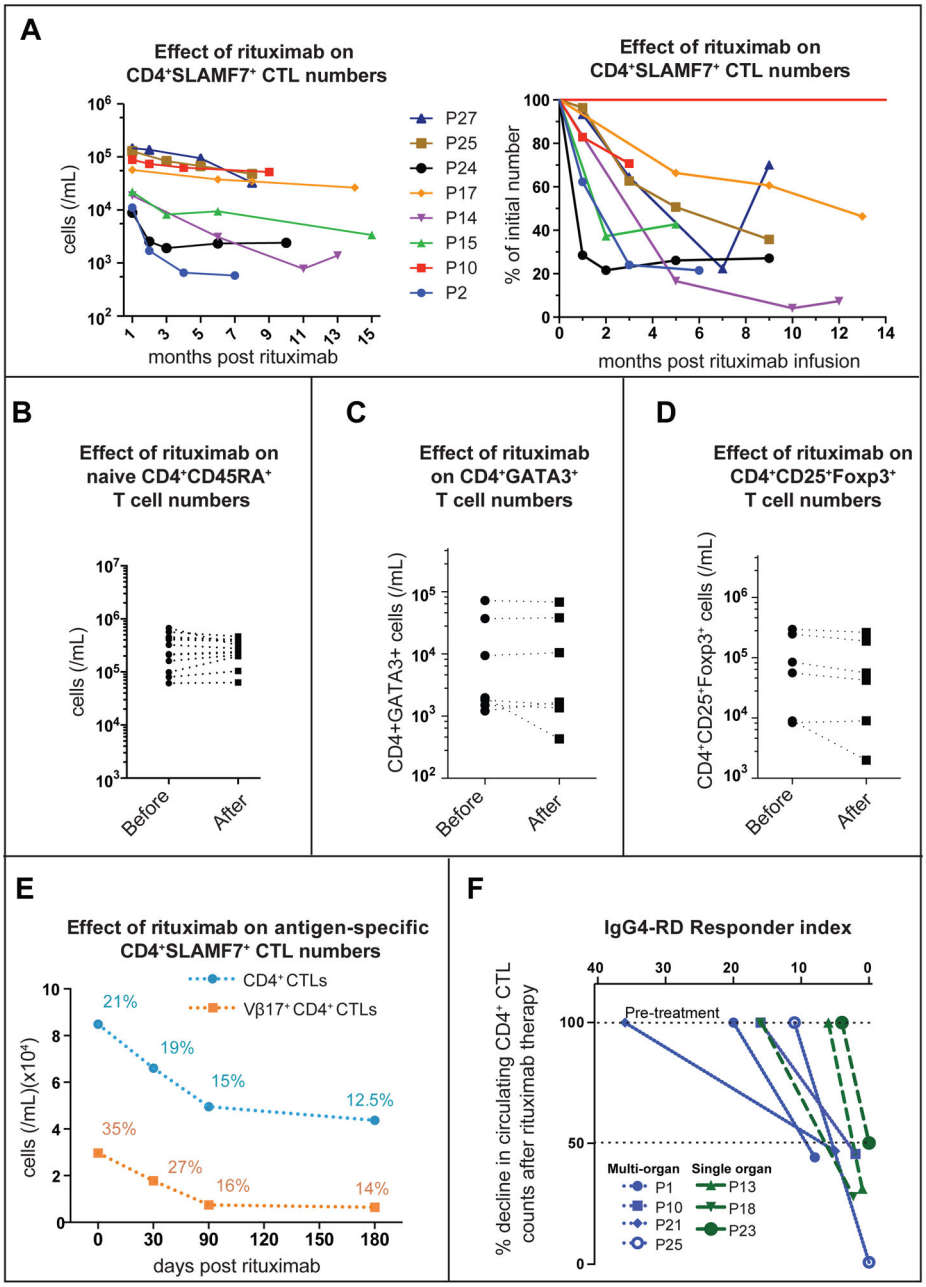

Figure 7. Rituximab-mediated depletion of CD4$^+$ CTLs

(A) Decline in CD4$^+$ SLAMF7$^+$ CTLs (n = 8 subjects) over 6–14 months following rituximab infusion shown as a change in cell counts and proportion.

(B) Effect of rituximab on CD4$^+$ CD45RA$^+$ naïve T cell counts in the peripheral blood of IgG4-RD patients.

(C & D) Effect of rituximab on CD4$^+$GATA-3$^+$ T_H2 cells and CD4$^+$CD25$^+$Foxp3$^+$ cells in the peripheral blood of IgG4-RD patients 90–120 days after rituximab therapy.

(E) Decline in the number and proportion of an expanded CD4$^+$ CTL clone tracked using a TCR-Vβ specific antibody following rituximab therapy in an IgG4-RD subject (P25).

(F) Decline in circulating $CD4^+$ CTL numbers at day 70–95 following rituximab therapy (normalized to the pretreatment levels) is plotted against the IgG4-RD Responder Index, a clinical measure of disease activity.

Table I

Overview of IgG4-RD subjects studied

Mean age at initial evaluation (mean +/− SD)	56.31 years (+/− 13.9)
Mean age at disease onset (mean +/− SD)	51.63 years (+/− 15.3)
% Male	61.4%
Race/Ethnicity	
% White	75%
% Black	6%
% Asian	11%
% Hispanic	6%
% Middle Eastern	2%
Serum IgG4 (Median, IQR) *	147.5 mg/dL (60.3 – 387)
% with Elevated Serum IgG4 at Baseline *	53.5%
Number of organs affected (mean +/− SD)	2.3 (+/− 1.4)
Organ Involvement	
% with type 1 IgG4-related pancreatitis	18.8%
% with Submandibular/Parotid Gland Disease	38.6%
% with orbital disease ***	19.8%
% with lymphadenopathy	34.7%
% with retroperitoneal fibrosis	14.9%
% with tubulointerstitial nephritis	11.9%
% with pulmonary disease	19.8%

* Among those with active disease

*** Including lacrimal gland involvement (dacryoadenitis)